Perivascular spaces and where to find them – MR imaging and evaluation methods

Perivaskuläre Räume und wo sie zu finden sind – MR-Bildgebung und Auswertungsmethoden

Authors
Svea Seehafer, Naomi Larsen, Schekeb Aludin, Olav Jansen, Lars-Patrick Andreas Schmill

Affiliations
Clinic for Radiology and Neuroradiology, University Hospital Schleswig-Holstein – Campus Kiel, Germany

Key words
perivascular spaces, glymphatic system, MR imaging

received 6.11.2023
accepted 20.12.2023
published online 26.2.2024

Bibliography
Fortschr Röntgenstr 2024; 196: 1029–1036
DOI 10.1055/a-2254-5651
ISSN 1438-9029

Georg Thieme Verlag KG, Rüdigerstraße 14, 70469 Stuttgart, Germany

Correspondence
Svea Seehafer
Klinik für Radiologie und Neuroradiologie, Universitätsklinikum Schleswig-Holstein, Arnold-Heller-Straße 3, 24105 Kiel, Germany
Tel.: +49/4 31/50 06 12 02
svea.seehafer@uksh.de

ABSTRACT

Background Perivascular spaces (synonym: Virchow-Robin spaces) were first described over 150 years ago. They are defined as the fluid-filled spaces surrounding the small penetrating cerebral vessels. They gained growing scientific interest especially with the postulation of the so-called glymphatic system and their possible role in neurodegenerative and neuroinflammatory diseases.

Methods PubMed was used for a systematic search with a focus on literature regarding MRI imaging and evaluation methods of perivascular spaces. Studies on human in-vivo imaging were included with a focus on studies involving healthy populations. No time frame was set. The nomenclature in the literature is very heterogeneous with terms like “large”, “dilated”, “enlarged” perivascular spaces whereas borders and definitions often remain unclear. This work generally talks about perivascular spaces.

Results This review article discusses the morphologic MRI characteristics in different sequences. With the continual improvement of image quality, more and tinier structures can be depicted in detail. Visual analysis and semi or fully automated segmentation methods are briefly discussed.

Conclusion If they are looked for, perivascular spaces are apparent in basically every cranial MRI examination. Their physiologic or pathologic value is still under debate.

Key Points

- Perivascular spaces can be seen in basically every cranial MRI examination.
- Primarily T2-weighend sequences are used for visual analysis. Additional sequences are helpful for distinction from their differential diagnoses.
- There are promising approaches for the semi or fully automated segmentation of perivascular spaces with the possibility to collect more quantitative parameters.

Citation Format

- Seehafer S, Larsen N, Aludin S et al. Perivascular spaces and where to find them – MRI imaging and evaluation methods. Fortschr Röntgenstr 2024; 196: 1029–1036

ZUSAMMENFASSUNG

Hintergrund Perivaskuläre Räume (Synonym: Virchow-Robin-Räume) wurden erstmals vor bereits über 150 Jahren beschrieben. Sie sind definiert als der flüssigkeitsgefüllte Raum in Umgebung der kleinen penetrierenden zerebralen Gefäße. Zunehmendes wissenschaftliches Interesse erlangten sie insbesondere mit der Postulation des sogenannten glymphatischen Systems und ihrer möglichen Bedeutung bei neurodegenerativen und -inflammatorischen Erkrankungen.

Methoden Es erfolgte eine gezielte PubMed-Recherche mit Fokus auf Arbeiten zur MR-Bildgebung und Auswertung von perivaskulären Räumen. Eingeschlossen wurden Arbeiten zur humanen in-vivo Bildgebung. Insbesondere auf Arbeiten zur gesunden Bevölkerung wurde geachtet. Eine Zeitraumbegrenzung erfolgte nicht. Die Nomenklatur in der Literatur ist sehr heterogen. Häufig wird beispielsweise von „large“, „dilated“, „enlarged“ perivaskulären Räumen gesprochen, wobei Grenzen und Definitionen meist unklar sind. In der vorliegenden Arbeit wird daher allgemein die Bezeichnung „Perivaskuläre Räume“ verwendet.

Ergebnisse Der vorliegende Übersichtsartikel erörtert die MR-morphologischen Charakteristika perivaskulärer Räume in verschiedenen Sequenzen. Mit der sich stetig verbessernden Bildqualität können auch zunehmend kleinere Strukturen immer detaillierter visualisiert werden. Es werden sowohl die Methoden der visuellen Auswertung als auch der semi- oder vollautomatischen Segmentierung kurz erläutert.

Schlussfolgerung Perivaskuläre Räume sind in quasi jeder kraniellen MRT-Untersuchung sichtbar, wenn man ihnen Beachtung schenkt. Ihr physiologischer oder pathologischer Wert ist weiterhin wissenschaftlicher Diskussionsgegenstand.

Introduction and historical context

In recent years the significance of perivascular spaces (PVS) has increasingly become a topic of clinical and scientific interest. However, the first descriptions of PVS date back over 150 years. They were first observed and mentioned for the first time in 1843 by the French physician Durand-Fardel in his paper "Traité du ramollissement du cerveau". In an autopsy report he described a "état criblé" consisting of sieve-like small holes in the brain, primarily in the white matter and in the corpus striatum [1] (▶ **Fig. 1**). These spaces were initially called Virchow-Robin spaces in reference to the two pathologists Virchow and Robin. In 1851, in the article "Ueber die Erweiterung kleinerer Gefäße", the German pathologist Virchow described a space in the vascular wall between the tunica intima/media and the tunica adventitia and called it "dissecting ectasia" [2]. In 1859, in his article "recherches sur quelques particularités de la structure des capillaires de l'encéphale", the French anatomist Robin described a closed space within the tunica adventitia [3]. These spaces were described as non-pathological findings in both publications. Today, PVS are defined as fluid-filled spaces surrounding small penetrating cerebral vessels.

Particularly in connection with the model of cerebral clearance by the glial-lymphatic ("glymphatic") system [4], PVS increasingly became the focus of scientific interest. It is hypothesized that these spaces play a central role in the drainage system of the central nervous system and are thus involved in the removal of metabolic waste products. It is therefore also postulated that they could serve as biomarkers for brain health and disease. A connection with neurodegenerative diseases like Alzheimer's or Parkinson's disease is suspected. Magnetic resonance imaging (MRI) as a noninvasive imaging method allows detailed in-vivo visualization of components of the glymphatic system like the perivascular spaces. The goal of this review is therefore to provide an overview of MR imaging of perivascular spaces and to give a summary of the various assessment methods in order to determine relevant points for the clinical routine.

MRI and characteristics of perivascular spaces in various sequences

PVS can be visualized in almost every cranial MRI examination in routine sequences due to the constant improvements in the spatial resolution of modern scanners [5].

In particular, T2-weighted (T2w) TSE sequences provide a high contrast-to-noise ratio (CNR) for the visualization of perivascular spaces [6]. Additional sequences can further facilitate the differentiation between perivascular spaces and their differential diagnoses (▶ **Tab. 1**). In the region of the basal ganglia (BG), the PVS run along the lenticulostriate vessels. Continuity to the basal cisterns can be observed. In the centrum semiovale (CSO), they begin several millimeters below the cortex [6, 7]. Tractography with diffusion tensor imaging shows that the PVS and their central vessels run parallel to the axons of the white matter [8]. In T2w and balanced steady-state free precession (bSSFP) sequences, ependymal openings and thus direct connections to the ventricular system could be detected in the periventricular PVS. The openings are largely located in the basal lateral wall of the anterior horn of the lateral ventricle [9]. In the midbrain, they are seen on highly T2w images at the pontomesencephalic junction mainly between the cerebral peduncles and the substantia nigra. At the diencephalic-mesencephalic junction, PVS are mainly located dorsal to the cerebral peduncles and are significantly smaller [10] (▶ **Fig. 2a**). To date, studies have only been able to examine

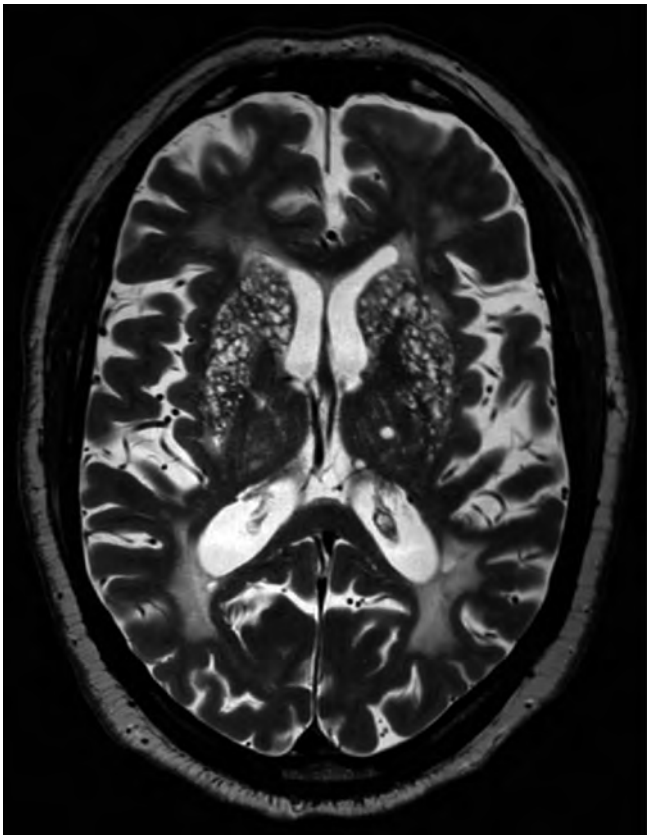

▶ **Fig. 1** "état criblé": axial T2-weighted sequence with multiple enlarged perivascular spaces at the level of the basal ganglia.

▶ **Table 1** Characteristics of perivascular spaces in different MRI-sequences.

Sequence	Characteristics of perivascular spaces	Comment
T2w	Hyperintense, clear margins Oblong when the course is parallel to the slice/round-oval when the course is perpendicular to the slice	Standard sequence for visual assessment in axial view
T1w	Hypointense, clear margins	
EPC	Hypointense	Delimitation from vessels without surrounding perivascular spaces; these are hyperintense here
FLAIR	Hypointense, clear margins	Delimitation from differential diagnoses (e. g., WMH, gliosis, and small lacunae)
TOF, SWI/T2*	No signal in the TOF sequence No SWI changes	Relation to arterial and venous vessels
DWI	No diffusion restrictions	Calculation of the DWI-ALPS index
DTI		Tractography for correlation to the course of the perivascular spaces Calculation of the DTI-ALPS index

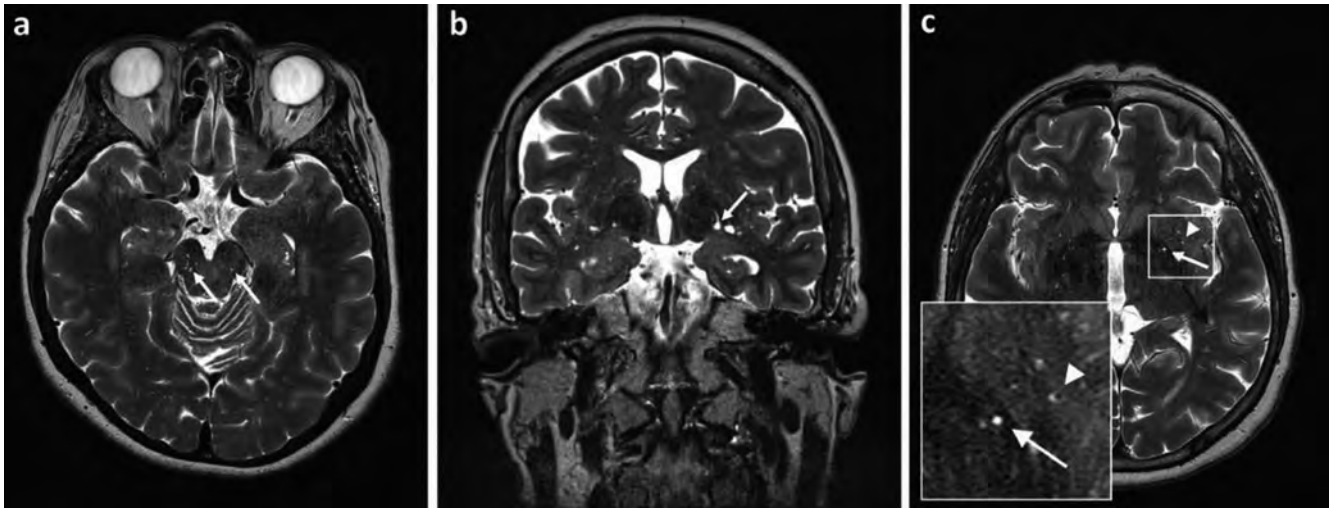

▶ **Fig. 2** **a** axial T2-weighted sequence at the level of the midbrain. The arrows indicate perivascular spaces on both sides. **b** coronal T2-weighted sequence at the level of the basal ganglia. The arrow indicates focal dilatation of a perivascular space. **c** axial T2-weighted sequence at the level of the basal ganglia. The white arrow shows a round-ovoid course. The black arrow shows a linear course. The white arrowhead indicates a central vessel in a perivascular space.

some PVS within the cortex ex vivo using 7 T devices [11]. They may become dilated in histological specimens during the fixation process and be significantly smaller in vivo than in white matter so that the spatial resolution of MRI or the CNR is too low.

Depending on the image plane, PVS appear either linear or oval since they follow the course of the penetrating vessels [12], with the possibility of focal dilation and fluctuations in caliber [6, 7] (▶ **Fig. 2b**).

It has been reported that PVS usually have a spatial relationship to the perforating arteries. Depending on the proportion between vascular diameter and the fluid filling the PVS, the central vessels within the PVS can sometimes be visualized (▶ **Fig. 2c**), e. g., on T1-weighted images after contrast administration [13] or in TOF angiography after contrast administration [14]. However, PVS are also seen without a corresponding artery and arteries are seen without corresponding PVS [7]. Some studies with an additional T2*-weighted or gradient echo/susceptibility-weighted (SWI) sequence also show that they do not or only minimally spatially correlate with the course of venous vessels [7, 15]. It is not yet clear whether this is due to a smaller size or different structure of the perivenous PVS. It is also conceivable that these are collapsed due to the lower pressure so that they are usually not visible. However, complete absence of perivenous PVS is also conceivable. Though, other studies with coregistered T2w and SWI sequences were able to show a perivenous location of at least a small portion of perivascular spaces [16].

Visually the signal of PVS is isointense with respect to CSF and is therefore completely suppressed in FLAIR sequences. In con-

trast to white matter hyperintensities (WMH), they are hypointense and do not have a hyperintense margin unless they are not within such a lesion [17]. However, the measured signal intensity of PVS has a low hyperintensity compared to CSF which indicates different compositions [18] that have not yet been sufficiently examined. Further studies also show signal differences between perivascular spaces of different regions thus also indicating variations in fluid composition [19].

After intravenous administration of gadolinium-based contrast agent, PVS along the perforating arteries and in the BG show significant enhancement on highly T2w FLAIR images after approximately three or four hours [20, 21]. In contrast, no comparable effect was observed in the PVS of the white matter in the subinsular region [19]. One possible reason for this could be different drainage routes and functions between PVS in various regions.

The combination of MRI sequences with different weightings could further increase the visibility of PVS in the future. The enhanced perivascular space contrast (EPC), a combination of T1w and T2w sequences, was established for this. Due to the inverse signal behavior of fluid here, a combination of these sequences results in greater contrast between PVS and tissue. A further advantage of this method is the differentiation of vessels with and without surrounding PVS. Without PVS, vessels are hypointense in the T2w sequence and hyperintense in the EPC. With surrounding PVS, vessels are hyperintense in the T2w sequence and hypointense in the EPC [22].

To determine the activity of the glymphatic system, Taoka et al. evaluated the diffusion tensor image analysis along the perivascular space (DTI-ALPS). The ALPS index is the ratio of the diffusivity along the PVS to the diffusivity along the projection and association fibers of a slice [23].

The same group also used their method for simple diffusion-weighted imaging. ADC maps can be generated from DWI sequences on the axes described above. The DWI-ALPS index can then be calculated in the same slice [24].

Perivascular spaces over the course of a lifetime and in health and disease

Studies show that PVS become more visible with increasing age [7]. Whether there are also changes in diameter is still a topic of discussion. The underlying mechanisms are debated in the literature. Studies show that there is a hereditary component [25]. It seems that men have a higher number of perivascular spaces [26]. Prospective studies were able to show that PVS are associated with age, lacunar infarcts, and white matter lesions. Therefore, they are increasingly being seen as further markers of cerebral small vessel disease [27]. A positive correlation between the number of PVS and white matter lesions is also seen in *cerebral autosomal dominant arteriopathy with subcortical infarcts and leukoencephalopathy* (CADASIL) as a monogenetic and early-onset form of cerebral small vessel disease [28]. Various PVS patterns could be detected in the case of spontaneous intracerebral bleeding. Thus the prevalence of PVS in the BG appears to be associated with hypertensive bleeding and the presence of PVS in the CSO appears to be associated with bleeding in cerebral amyloid angiopathy [29]. A further genetic disease involving dilation of the PVS is, for example, mucopolysaccharidosis, which as a lysosomal storage disease is associated with manifestations in the CNS among other things. PVS are seen here primarily in unusual locations, e. g., along the junction zone between gray and white matter. However, there is no correlation with cognitive performance [30]. Even if the available data is still contradictory, the burden on PVS seems to correlate with neurodegenerative diseases like multiple sclerosis, Alzheimer's disease, and Parkinson's disease. The underlying mechanisms continue to be the subject of research. The correlation between PVS and cognitive performance is also controversial in the current literature.

Visual assessment

In relation to the visual scoring of PVS, the increasing number of publications has resulted in a corresponding increase in the number of assessment methods.

A classification based on the distribution of PVS includes three characteristic locations: Type I along the perforating lenticulostriate arteries in the BG, type II along the perforating subcortical white matter arteries above the convexity, and type III in the midbrain at the pontomesencephalic junction [31]. A type IV was recently suggested for the subcortical white matter of the anterior superior temporal gyrus [32]. However, PVS can occur anywhere in the brain parenchyma.

Grading of the PVS based on size is sometimes used. To date, there is no standardized definition here. In an early study, grade 1 was defined for a diameter of < 2 mm, grade 2 for a diameter of 2–3 mm, and grade 3 for a diameter of > 3 mm [33]. Other studies define a lower limit of 1 mm [34] or 5 mm [31]. However, it is largely agreed that PVS < 3 mm are not considered dilated. In the case of larger PVS, differential diagnoses like lacunar infarcts must be taken into consideration [34–36]. In addition, the literature includes cases with so-called giant tumefactive perivascular spaces with dimensions of greater than 1.5 cm (▶ **Fig. 3a, b**). However, in spite of their size, they can be asymptomatic and an incidental finding [38]. They can also be associated with numerous symptoms and cause focal mass effects and even obstructive hydrocephalus [37]. In rare cases dilated PVS can be reversible, either in association with the resection or regression of cerebral lesions or spontaneously [13].

More recent studies define dilation of the PVS in the supratentorial white matter not based on diameter but rather on shape. The only differentiation is "not dilated" when they have an even and linear course and "dilated" in the case of visible irregularities or focal ectasia. According to the authors, this classification should have the advantage that it is easier to use and the size does not need to be normalized to the individual brain volume. Therefore, grading is less dependent on technical parameters [36].

To evaluate the quantity of dilated perivascular spaces, they can be counted in the various regions and applied to the rating.

The most established scale in studies with visual assessment of PVS in BG and CSO ranges from 0 to 4 with 0 = no PVS, 1 = 1–10, 2 = 11–20, 3 = 21–40, and 4 = > 40. This scale is used for both

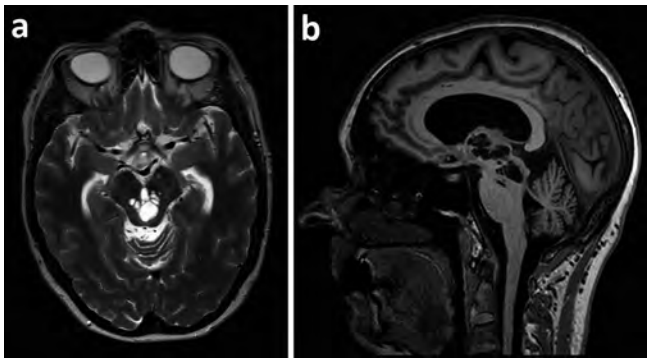

▶ **Fig. 3** giant tumefactive perivascular spaces **a** axial T2-weighted sequence. **b** sagittal T1-weigted sequence.

hemispheres. In the case of asymmetry, the higher score is used (▶ **Fig. 4**) [39]. For the mesencephalon, scores of 0 = not visible and 1 = visible are used [39].

The unclear number of assessment methods results in limited comparability between the studies to date. The goal of the "Uniform Neuro-Imaging of Virchow-Robin Spaces Enlargement" (UNIVERSE) consortium therefore is to harmonize the visual assessment of PVS and to make it more time efficient. Four relevant brain regions were defined: the CSO, the BG, the hippocampus, and the mesencephalon. For the first two regions, the perivascular spaces are counted in a predefined plane, while all perivascular spaces are counted in the last two perivascular spaces [4].

As described above, there is increasing evidence that both PVS and WMH are biomarkers for cerebral microvascular integrity and they are correlated with each other [26]. Initial approaches consider the two parameters together with a combined score. The ratings for perivascular spaces of the BG, the CSO, and the midbrain and the Fazekas score [41] are added [42].

Even if studies report good interobserver reliability of their visual scores, manual assessment is very time-intensive and subjectivity of the observers cannot be eliminated. The scores are often difficult to compare and are thus not suitable for longitudinal studies. It must also be clarified whether the continuously improving technology with higher field strengths and better resolution changes the detectability of PVS. Therefore, it is necessary to question whether the visual rating scales used to date also need to be adapted.

Automatic evaluation

A growing number of studies are addressing the semi-automatic or fully automatic analysis of PVS. The increasing number of studies has resulted in an increasing number of assessment methods. Therefore, there are multiple filter and segmentation methods that can potentially be applied to PVS. Initial approaches explicitly for segmenting PVS were seen in the early 2000 s when Descombes et al. first used a "marked point process framework" optimized via "reversible jump Markov chain Monte Carlo algorithm" to detect multiple small lesions [43].

These methods can roughly be divided into image processing for increasing the visibility of PVS and methods using artificial intelligence, deep learning algorithms in this case, with some overlap. Preprocessing to create a mask by segmenting gray and white matter and CSF and if necessary any subcortical structures is usually first performed.

For image processing, subgroups can be defined like intensity-based filter methods, which assign voxels to the PVS on the basis of intensity differences, and the Vesselness filter methods, which are used to identify tubular structures.

Early approaches were based on semi-automatic intensity-based segmentation in a predefined slice through the BG [44]. The following studies performed edge detection and processing of voxel-specific, high positive spatial gradients using the MATLAB "imgradient" function [8] in various regions [45].

A further study developed a method of Voxel-based multimodal autoidentification of PVS that performs automatic analysis and allocation of Voxels based on normalized signal intensities of the gray and white matter and the ventricular system in spatially coregistered T1w, FLAIR, T2w and PDw sequences [46]. An approach based on this by the same work group used only T1w and FLAIR sequences in order to reduce the acquisition time and to minimize the effect of movement between coregistered sequences [47].

Other studies used Vesselness filter methods like the Frangi filter [48]. Since the goal of this method is to show tubular structures, it can be effectively used for the visualization of PVS. PVS were defined here as tubular structures with a length of 3–50 mm [49]. Further studies using the Frangi filter with slight changes have been performed [6]. The filter can be used for T1w, T2w, and EPC images. The threshold values need to be adapted to the applied image and they must have the same resolution. The PVS can then be counted based on the resulting mask [22].

In addition to the Frangi filter, there are other filters like the Jerman filter and the RORPO filter based on morphological path operators. Which filters are used, for example in studies, depends on whether a high sensitivity or specificity or a high positive or negative predictive value is targeted [50].

A combination of the two methods mentioned above is also possible. For instance, Vesselness filters were applied in a study to highlight all vessel-like structures on T2w images. To automatically detect the PVS in a predefined slice, probability maps based on a binary kNN classification (k-nearest neighbor) were used [51].

With the further development of artificial intelligence, DL algorithms were also developed for the segmentation of PVS. However, a large number of manually annotated data sets are typically needed The visual PVS scores described above are ultimately usually used as a ground truth. However, a certain amount of data sets are still needed for training and validation. For example, "random forest" models [52, 53] or "convolutional neural networks" (CNN) [11, 54–56] are used as the basis for such approaches.

Since as described above the 4 main regions are the midbrain, hippocampus, BG, and CSO, one study designed an automatic quantification method for these regions. The approach used in this method is based on the CNN regression, which was designed for the detection of small objects within a region of interest. Due to the potentially different shapes and differential diagnoses of

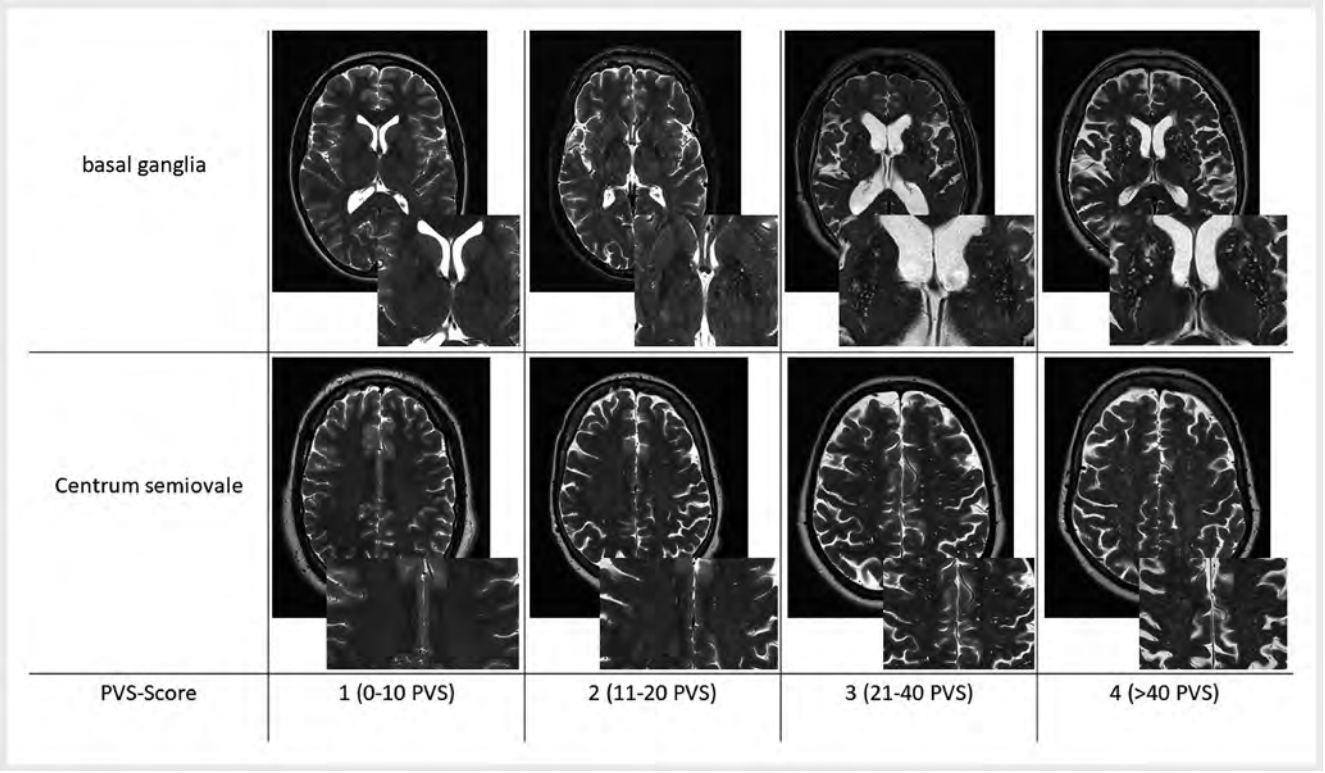

▶ **Fig. 4** Visual score for rating of perivascular spaces at the level of the basal ganglia (upper row) and at the level of the centrum semiovale (bottom row) on axial T2-weighted images. All images were acquired with a 3T-MRI scanner (MAGNETOM Vida 3 T, Siemens Healthcare, Erlangen, Germany).

PVS in these areas, the CNN was trained specifically for these regions [57].

The DL methods can also be combined, e. g., with Frangi filter and CNN-based classification via 3 D deep CNN [25].

Automatic methods are capable of detecting a high number of even very small PVS thus allowing deeper analyses. Therefore, quantitative parameters like an exact count or the diameter of PVS can be determined [6]. Furthermore, the length and individual PVS volume can be calculated, which can then be corrected as a volume fraction for the entire brain volume [8, 45]. Morphological differences like linearity [46] and shape between regions can also be examined potentially more objectively.

Automatic PVS assessment is still in the initial phase and it is difficult to compare the different approaches due to the various sequences and devices with different field strengths. To actively promote research in this field, the Medical Image Computing and Computer-Assisted Interventions Association (MICCAI) started the Vascular Lesions Detection (VALDO) Challenge in 2021. The detection of PVS is a subcategory: Better comparability is desired since proposals are evaluated based on the same guidelines and data sets. (https://valdo.grand-challenge.org/).

Summary

PVS are visible in practically every cranial MRI examination even using routine clinical sequences. They are a normal finding in people without neurological abnormalities. However, their clinical relevance is not yet fully understood. To date, there is only minimal data from healthy persons to determine a cut-off between physiological and pathological. There are numerous scoring systems for visual assessment. Automatic segmentation is a promising approach for standardizing findings and ensuring comparability between studies.

Conflict of Interest

The authors declare that they have no conflict of interest.

References

[1] Durand-Fardel M. Traite du ramollissement du cerveau. Paris: Balliere; 1843

[2] Virchow R. Ueber die Erweiterung kleinerer Gefäße; 1851

[3] Robin Ch. Recherches sur quelques particularités de la structure des capillaires de l'encéphale, Journal de physiologie; 1859

[4] Iliff JJ, Wang M, Liao Y et al. A paravascular pathway facilitates CSF flow through the brain parenchyma and the clearance of interstitial solutes, including amyloid β. Sci Transl Med 2012; 4: 147ra111. doi:10.1126/scitranslmed.3003748

[5] Zhu Y-C, Dufouil C, Mazoyer B et al. Frequency and location of dilated Virchow-Robin spaces in elderly people: a population-based 3D MR imaging study. AJNR Am J Neuroradiol 2011; 32: 709–713. doi:10.3174/ajnr.A2366

[6] Zong X, Park SH, Shen D et al. Visualization of perivascular spaces in the human brain at 7T: sequence optimization and morphology characterization. Neuroimage 2016; 125: 895–902. doi:10.1016/j.neuroimage.2015.10.078

[7] Bouvy WH, Biessels GJ, Kuijf HJ et al. Visualization of Perivascular Spaces and Perforating Arteries With 7 T Magnetic Resonance Imaging. Invest Radiol 2014; 49: 307–313. doi:10.1097/RLI.0000000000000027

[8] Cai K, Tain R, Das S et al. The feasibility of quantitative MRI of perivascular spaces at 7T. J Neurosci Methods 2015; 256: 151–156. doi:10.1016/j.jneumeth.2015.09.001

[9] Tsutsumi S, Ono H, Ishii H et al. Visualization of the periventricular Virchow-Robin spaces with ependymal openings. Childs Nerv Syst 2018; 34: 1529–1533. doi:10.1007/s00381-018-3793-y

[10] Saeki N, Sato M, Kubota M et al. MR imaging of normal perivascular space expansion at midbrain. AJNR Am J Neuroradiol 2005; 26 (3): 566–571

[11] Perosa V, Oltmer J, Munting LP et al. Perivascular space dilation is associated with vascular amyloid-β accumulation in the overlying cortex. Acta Neuropathol 2022; 143: 331–348. doi:10.1007/s00401-021-02393-1

[12] Wardlaw JM, Smith EE, Biessels GJ et al. Neuroimaging standards for research into small vessel disease and its contribution to ageing and neurodegeneration. The Lancet Neurology 2013; 12: 822–838. doi:10.1016/S1474-4422(13)70124-8

[13] Cerase A, Vallone IM, Muccio CF et al. Regression of dilated perivascular spaces of the brain. Surg Radiol Anat 2010; 32: 555–561. doi:10.1007/s00276-009-0603-y

[14] Taydas O, Erarslan Y, Ates OF et al. Tumefactive perivascular space demonstrated with post-contrast time-of-flight MR angiography. Neurochirurgie 2020; 66: 50–52. doi:10.1016/j.neuchi.2019.11.003

[15] Jochems ACC, Blair GW, Stringer MS et al. Relationship Between Venules and Perivascular Spaces in Sporadic Small Vessel Diseases. Stroke 2020; 51: 1503–1506. doi:10.1161/STROKEAHA.120.029163

[16] George IC, Arrighi-Allisan A, Delman BN et al. A Novel Method to Measure Venular Perivascular Spaces in Patients with MS on 7T MRI. AJNR Am J Neuroradiol 2021; 42: 1069–1072. doi:10.3174/ajnr.A7144

[17] Awad IA, Johnson PC, Spetzler RF et al. Incidental subcortical lesions identified on magnetic resonance imaging in the elderly. II. Postmortem pathological correlations. Stroke 1986; 17: 1090–1097. doi:10.1161/01.str.17.6.1090

[18] Oztürk MH, Aydingöz U. Comparison of MR signal intensities of cerebral perivascular (Virchow-Robin) and subarachnoid spaces. J Comput Assist Tomogr 2002; 26: 902–904. doi:10.1097/00004728-200211000-00008

[19] Naganawa S, Nakane T, Kawai H et al. Differences in Signal Intensity and Enhancement on MR Images of the Perivascular Spaces in the Basal Ganglia versus Those in White Matter. Magn Reson Med Sci 2018; 17: 301–307. doi:10.2463/mrms.mp.2017-0137

[20] Deike-Hofmann K, Reuter J, Haase R et al. Glymphatic Pathway of Gadolinium-Based Contrast Agents Through the Brain: Overlooked and Misinterpreted. Invest Radiol 2019; 54: 229–237. doi:10.1097/RLI.0000000000000533

[21] Naganawa S, Nakane T, Kawai H et al. Gd-based Contrast Enhancement of the Perivascular Spaces in the Basal Ganglia. Magn Reson Med Sci 2017; 16: 61–65. doi:10.2463/mrms.mp.2016-0039

[22] Sepehrband F, Barisano G, Sheikh-Bahaei N et al. Image processing approaches to enhance perivascular space visibility and quantification using MRI. Sci Rep 2019; 9. doi:10.1038/s41598-019-48910-x

[23] Taoka T, Masutani Y, Kawai H et al. Evaluation of glymphatic system activity with the diffusion MR technique: diffusion tensor image analysis along the perivascular space (DTI-ALPS) in Alzheimer's disease cases. Jpn J Radiol 2017; 35: 172–178. doi:10.1007/s11604-017-0617-z

[24] Taoka T, Ito R, Nakamichi R et al. Diffusion-weighted image analysis along the perivascular space (DWI-ALPS) for evaluating interstitial fluid status: age dependence in normal subjects. Jpn J Radiol 2022; 40: 894–902. doi:10.1007/s11604-022-01275-0

[25] Choi Y, Nam Y, Choi Y et al. MRI-visible dilated perivascular spaces in healthy young adults: A twin heritability study. Hum Brain Mapp 2020; 41: 5313–5324. doi:10.1002/hbm.25194

[26] Zhu Y-C, Tzourio C, Soumaré A et al. Severity of dilated Virchow-Robin spaces is associated with age, blood pressure, and MRI markers of small vessel disease: a population-based study. Stroke 2010; 41: 2483–2490. doi:10.1161/STROKEAHA.110.591586

[27] Potter GM, Doubal FN, Jackson CA et al. Enlarged Perivascular Spaces and Cerebral Small Vessel Disease. International Journal of Stroke 2015; 10: 376–381. doi:10.1111/ijs.12054

[28] Rajani RM, Ratelade J, Domenga-Denier V et al. Blood brain barrier leakage is not a consistent feature of white matter lesions in CADASIL. Acta Neuropathol Commun 2019; 7: 187. doi:10.1186/s40478-019-0844-x

[29] Charidimou A, Boulouis G, Pasi M et al. MRI-visible perivascular spaces in cerebral amyloid angiopathy and hypertensive arteriopathy. Neurology 2017; 88: 1157–1164. doi:10.1212/WNL.0000000000003746

[30] Gabrielli O, Polonara G, Regnicolo L et al. Correlation between cerebral MRI abnormalities and mental retardation in patients with mucopolysaccharidoses. Am J Med Genet A 2004; 125A: 224–231. doi:10.1002/ajmg.a.20515

[31] Kwee RM, Kwee TC. Virchow-Robin spaces at MR imaging. Radiographics 2007; 27: 1071–1086. doi:10.1148/rg.274065722

[32] Rawal S, Croul SE, Willinsky RA et al. Subcortical cystic lesions within the anterior superior temporal gyrus: a newly recognized characteristic location for dilated perivascular spaces. AJNR Am J Neuroradiol 2014; 35: 317–322. doi:10.3174/ajnr.A3669

[33] Heier LA, Bauer CJ, Schwartz L et al. Large Virchow-Robin spaces: MR-clinical correlation. AJNR Am J Neuroradiol 1989; 10: 929–936

[34] Adams HHH, Cavalieri M, Verhaaren BFJ et al. Rating method for dilated Virchow-Robin spaces on magnetic resonance imaging. Stroke 2013; 44: 1732–1735. doi:10.1161/STROKEAHA.111.000620

[35] Jungreis CA, Kanal E, Hirsch WL et al. Normal perivascular spaces mimicking lacunar infarction: MR imaging. Radiology 1988; 169: 101–104. doi:10.1148/radiology.169.1.3420242

[36] Groeschel S, Chong WK, Surtees R et al. Virchow-Robin spaces on magnetic resonance images: normative data, their dilatation, and a review of the literature. Neuroradiology 2006; 48: 745–754. doi:10.1007/s00234-006-0112-1

[37] Salzman KL, Osborn AG, House P et al. Giant tumefactive perivascular spaces. AJNR Am J Neuroradiol 2005; 26 (2): 298–305

[38] Idiculla PS, Gurala D, Siddiqui JH. Giant tumefactive perivascular spaces: an incidental finding. Acta Neurol Belg 2020; 120: 1443–1444. doi:10.1007/s13760-020-01481-5

[39] Potter GM, Chappell FM, Morris Z et al. Cerebral perivascular spaces visible on magnetic resonance imaging: development of a qualitative rating scale and its observer reliability. Cerebrovasc Dis 2015; 39: 224–231. doi:10.1159/000375153

[40] Adams HH, Hilal S, Schwingenschuh P et al. A priori collaboration in population imaging: The Uniform Neuro-Imaging of Virchow-Robin Spaces Enlargement consortium. Alzheimer's & Dementia: Diagnosis, Assessment & Disease Monitoring 2015; 1: 513–520. doi:10.1016/j.dadm.2015.10.004

[41] Fazekas F, Chawluk JB, Alavi A et al. MR signal abnormalities at 1.5 T in Alzheimer's dementia and normal aging. American Journal of Roentgenology 1987; 149: 351–356. doi:10.2214/ajr.149.2.351

[42] Zdanovskis N, Platkājis A, Kostiks A et al. Combined Score of Perivascular Space Dilatation and White Matter Hyperintensities in Patients with Normal Cognition, Mild Cognitive Impairment, and Dementia. Medicina (Kaunas) 2022; 58. doi:10.3390/medicina58070887

[43] Descombes X, Kruggel F, Wollny G et al. An object-based approach for detecting small brain lesions: application to Virchow-Robin spaces. IEEE Trans Med Imaging 2004; 23: 246–255. doi:10.1109/TMI.2003.823061

[44] Wang X, Del Valdés Hernández MC, Doubal F et al. Development and initial evaluation of a semi-automatic approach to assess perivascular spaces on conventional magnetic resonance images. J Neurosci Methods 2016; 257: 34–44. doi:10.1016/j.jneumeth.2015.09.010

[45] Niazi M, Karaman M, Das S et al. Quantitative MRI of Perivascular Spaces at 3T for Early Diagnosis of Mild Cognitive Impairment. AJNR Am J Neuroradiol 2018; 39: 1622–1628. doi:10.3174/ajnr.A5734

[46] Boespflug EL, Schwartz DL, Lahna D et al. MR Imaging-based Multimodal Autoidentification of Perivascular Spaces (mMAPS): Automated Morphologic Segmentation of Enlarged Perivascular Spaces at Clinical Field Strength. Radiology 2018; 286: 632–642. doi:10.1148/radiol.2017170205

[47] Schwartz DL, Boespflug EL, Lahna DL et al. Autoidentification of perivascular spaces in white matter using clinical field strength T1 and FLAIR MR imaging. Neuroimage 2019; 202: 116126. doi:10.1016/j.neuroimage.2019.116126

[48] Frangi A, Niessen W, Vincken K et al. M. Multiscale vessel enhancement filtering. Medical Image Computing and Computer-Assisted Intervention (MICCAI98); 1998: 130–137

[49] Ballerini L, Lovreglio R, Del Valdés Hernández MC et al. Perivascular Spaces Segmentation in Brain MRI Using Optimal 3D Filtering. Sci Rep 2018; 8: 2132. doi:10.1038/s41598-018-19781-5

[50] Bernal J, Valdés-Hernández MDC, Escudero J et al. Assessment of perivascular space filtering methods using a three-dimensional computational model. Magn Reson Imaging 2022; 93: 33–51. doi:10.1016/j.mri.2022.07.016

[51] Spijkerman JM, Zwanenburg J, Bouvy WH et al. Automatic quantification of perivascular spaces in T2-weighted images at 7 T MRI. Cerebral Circulation – Cognition and Behavior 2022; 3: 100142. doi:10.1016/j.cccb.2022.100142

[52] Hou Y, Park SH, Wang Q et al. Enhancement of Perivascular Spaces in 7T MR Image using Haar Transform of Non-local Cubes and Block-matching Filtering. Sci Rep 2017; 7: 8569. doi:10.1038/s41598-017-09336-5

[53] Park SH, Zong X, Gao Y et al. Segmentation of perivascular spaces in 7T MR image using auto-context model with orientation-normalized features. Neuroimage 2016; 134: 223–235. doi:10.1016/j.neuroimage.2016.03.076

[54] Zhang J, Gao Y, Park SH et al. Structured Learning for 3-D Perivascular Space Segmentation Using Vascular Features. IEEE Trans Biomed Eng 2017; 64: 2803–2812. doi:10.1109/TBME.2016.2638918

[55] Boutinaud P, Tsuchida A, Laurent A et al. 3D Segmentation of Perivascular Spaces on T1-Weighted 3 Tesla MR Images With a Convolutional Autoencoder and a U-Shaped Neural Network. Front. Neuroinform 2021; 15. doi:10.3389/fninf.2021.641600

[56] Lian C, Zhang J, Liu M et al. Multi-channel multi-scale fully convolutional network for 3D perivascular spaces segmentation in 7T MR images. Med Image Anal 2018; 46: 106–117. doi:10.1016/j.media.2018.02.009

[57] Dubost F, Yilmaz P, Adams H et al. Enlarged perivascular spaces in brain MRI: Automated quantification in four regions. Neuroimage 2019; 185: 534–544. doi:10.1016/j.neuroimage.2018.10.026